Carbohydrate Research ■■ (2016) ■■–■■

Contents lists available at ScienceDirect

Carbohydrate Research

journal homepage: www.elsevier.com/locate/carres

Note

Voglibose-inspired synthesis of new potent α-glucosidase inhibitors *N*-1,3-dihydroxypropylaminocyclitols

Wisuttaya Worawalai, Pornthep Sompornpisut, Sumrit Wacharasindhu, Preecha Phuwapraisirisan *

Department of Chemistry, Faculty of Science, Chulalongkorn University, Bangkok 10330, Thailand

ARTICLE INFO

Article history:
Received 9 January 2016
Received in revised form 8 April 2016
Accepted 9 April 2016
Available online

Keywords:
Diabetes mellitus
Glucosidase
Voglibose
Cyclitol
Serinol
Quercitol

ABSTRACT

Voglibose, an *N*-1,3-dihydroxypropylaminocyclitol, has widely been used as an effective α-glucosidase inhibitor for diabetes therapy. Several attempts have been made to synthesize closely related analogues through the coupling of various aminocyclitols and propane-1,3-diol; however, most of them showed weaker or no inhibition. In this communication, we synthesized a pair of new *N*-1,3-dihydroxypropylaminocyclitols (**10** and **11**) using (+)-*proto*-quercitol (**1**) as a cyclitol core structure. The newly synthesized compounds revealed potent rat intestinal α-glucosidases, particularly against maltase, with IC_{50} values at submicromolar. Subsequent study on mechanisms underlying the inhibition of **11** indicated the competitive manner towards maltase and sucrase. The potent inhibition of these compounds was elaborated by docking study, in which their binding profiles towards key amino acid residues in the active site were similar to that of voglibose. Therefore, introduction of propane-1,3-diol moiety to suitable cyclohexane core structure such as aminoquercitol would be a potential approach to discover a new series of effective α-glucosidase inhibitors.

Effective control of hyperglycaemia is a critical approach for diabetes and its complication therapy. The high blood glucose level can be attenuated by inhibiting α-glucosidase, the enzyme catalyzing hydrolysis of oligosaccharide to glucose. To date, there have been three α-glucosidase inhibitors, namely acarbose, miglitol and voglibose, currently approved for hyperglycaemia control; of which voglibose is the newest and most effective. The outstanding efficacy of voglibose can be rationalized by its synergistic effects when applied together with different antidiabetic drugs. Plasma glucose control was improved in 65% of patients who exhibited a poor response to sulphonylurea while no major adverse effects were observed.[1] In comparison with acarbose (100 mg), voglibose at much lower dosage (0.2 mg) significantly decreased postprandial insulin and glucose levels with less gastrointestinal side effect.[2] In addition, voglibose has been used to improve glycaemic control by suppressing glycated haemoglobin (HbA1c) level at lower dose (0.6 mg) than miglitol (150 mg).[3] More interestingly, voglibose also showed hypoinsulinaemic and hypolipidaemic effects through improvement of insulin sensitivity.[4]

Since the launch of voglibose by Takeda Pharmaceutical Company in 1994, several attempts to synthesize voglibose-related analogues have been made. Noticeably, most derivatives were prepared from reductive amination of 2-amino-1,3-propanediol (commonly known as serinol) and polyhydroxycycloalkanones with larger ring size (Fig. 1). Le Merrer's group synthesized cycloheptane-aminocyclitol and a series of cyclooctane analogues,[5–10] in the hope that the flexibility of the larger ring and new spatial distribution of hydroxyl groups would enhance the inhibitory effect. However, most of them showed weaker or no inhibition against α-glucosidases. Although the critical role of serinol moiety in enzyme binding is not yet well understood, the cyclohexane-C1-aminocyclitols possessing this moiety are likely to reveal inhibition nearly equipotent to that of voglibose. The observed tendency is possibly associated with the fact that the cyclohexane-C1-aminocyclitols core structure is capable of mimicking the transition state of the enzyme-substrate complex while the serinol group on the nitrogen atom enhances tight binding with the active site. With this assumption in mind, we have the idea to introduce quercitol as the cyclohexane-cyclitol core structure of choice to synthesize new *N*-1,3-dihydroxypropylaminocyclitols. We hope that the lack of C1-residue ($-CH_2OH$) in the quercitol structure will not alter its inherent binding affinity to the active site of the enzyme.

Quercitol is a natural cyclitol possessing five contiguous hydroxyl groups in which (+)-*proto*-quercitol (**1**) is the most naturally abundant and widely applied in organic synthesis. The versatility of this building block has been demonstrated by a diverse series of quercitol-derived analogues.[11–13] Noticeably, functional group modification of (+)-*proto*-quercitol mostly afforded products with

* Corresponding author. Department of Chemistry, Faculty of Science, Chulalongkorn University, Bangkok 10330, Thailand. Tel.: +662 2187624; fax: +662 2187598.
E-mail address: preecha.p@chula.ac.th (P. Phuwapraisirisan).

http://dx.doi.org/10.1016/j.carres.2016.04.014
0008-6215/

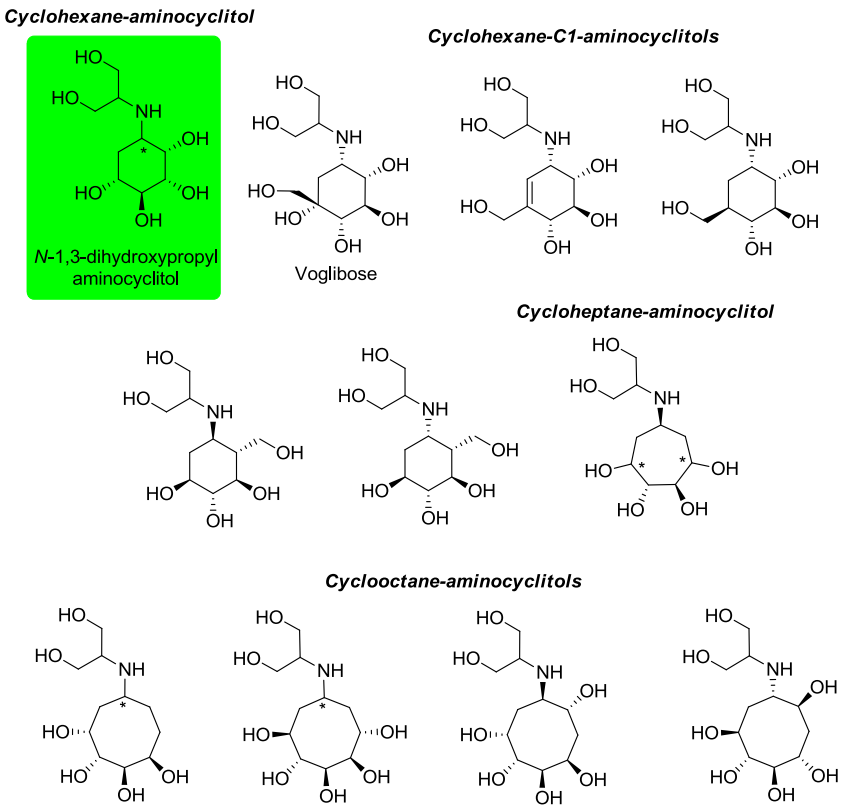

Fig. 1. Structures of *N*-1,3-dihydroxypropylaminocyclitols.

enhanced inhibition, therefore suggesting the good fit of the quercitol core structure to the active site of an enzyme. In this communication, we plan to synthesize new α-glucosidase inhibitors having (+)-*proto*-quercitol as the cyclitol core structure modified with serinol moiety. Furthermore, the inhibitory mechanism and computational study of the targeted compounds are herein described.

We designed the synthesis of the targeted *N*-1,3-dihydroxypropylaminocyclitols (**10** and **11**) through the reductive amination of aminoquercitol bisacetonides (**5** and **8**) and 1,3-dihydroxyacetone dimer (**9**) as shown in Scheme 1. The aminoquercitol bisacetonides **5** and **8** were prepared from naturally available (+)-*proto*-quercitol (**1**) using our protocol (Scheme 2) as previously described.[11] Initially, the hydroxy groups in **1** were protected by the reaction with $Me_2C(OMe)_2$ in the presence of *p*-TsOH, thus yielding bisacetonide **2** as a single product in 75% yield. The conversion of the remaining hydroxy moiety into the amino group in **2** was accomplished in three steps. Mesylation of **2** with $MeSO_2Cl$ generated the mesylate **3**. Nucleophilic substitution of the mesylate with azide occurred with inversion to yield **4**. Finally, reduction of the azide group using $LiAlH_4$ produced the desired aminoquercitol bisacetonide **5**.

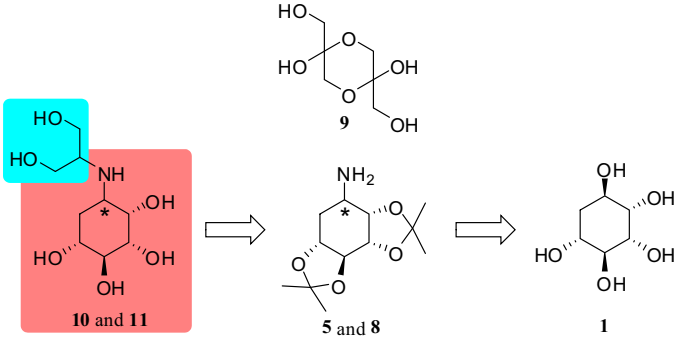

Scheme 1. Retrosynthesis of *N*-1,3-dihydroxypropylaminocyclitols (**10** and **11**).

With **5** in hand, we next planned to synthesize aminoquercitol bisacetonide **8** (Scheme 3), with the C-1 configuration of C-1 opposite to that of **5**. Starting from **2**, Albright–Goldman oxidation using Ac_2O/DMSO[14] afforded the corresponding ketone **6**. Subsequent reduction of the ketone furnished the hydroxybisacetonide **7** as a single product with excellent yield (93%). The expected aminoquercitol bisacetonide **8** was obtained using the same methodology applied for **2**.

Finally, the desired *N*-1,3-dihydroxypropylaminocyclitol **10** was synthesized by reductive amination between aminoquercitol bisacetonide **5** and 1,3-dihydroxyacetone dimer (**9**) in the presence of $NaBH_3CN$/AcOH (Scheme 4). In similar fashion, *N*-1,3-dihydroxypropylaminocyclitol **11** was also prepared from aminoquercitol bisacetonide **8** and 1,3-dihydroxyacetone dimer (**9**) using the above method.

The two *N*-1,3-dihydroxypropylaminocyclitols (**10** and **11**) were assessed as inhibitors of α-glucosidases from two different sources: baker's yeast and rat intestine. Both compounds were strong inhibitors of maltase (0.57–0.90 μM) and sucrase (1.7–2.1 μM) whereas the inhibition against yeast α-glucosidase was not observed. These results were similar to those observed for antidiabetic drugs voglibose. Noticeably, the opposite configuration at C-1 of **10** and **11** did not significantly alter enzyme inhibition. Conversely, the related analogues possessing larger cycloalkane rings (cycloheptane and cyclooctane; Table 1) revealed no inhibitory effect against α-glucosidase. The observed results preliminarily suggested that the six-membered aminocyclitol core structure is more pivotal than the larger and more flexible cycloheptane- and cyclooctane-cyclitols as earlier postulated by Le Merrer.[5–10] This observation suggests that

Please cite this article in press as: Wisuttaya Worawalai, Pornthep Sompornpisut, Sumrit Wacharasindhu, Preecha Phuwapraisirisan, Voglibose-inspired synthesis of new potent α-glucosidase inhibitors *N*-1,3-dihydroxypropylaminocyclitols, Carbohydrate Research (2016), doi: 10.1016/j.carres.2016.04.014

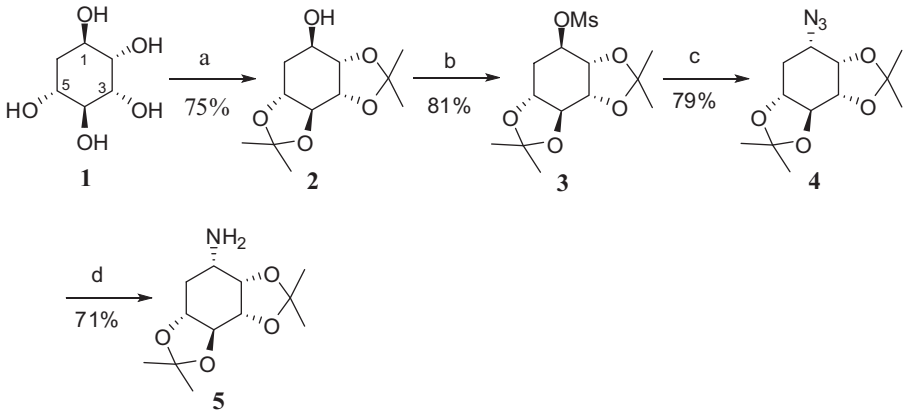

Scheme 2. Synthesis of aminoquercitol bisacetonide **5**. *Reagents and conditions*: (a) $Me_2C(OMe)_2$, DMF, *p*–TsOH; (b) $MeSO_2Cl$, Et_3N, DMAP; (c) NaN_3, DMF, 15-crown-5-ether, 100 °C; (d) $LiAlH_4$.

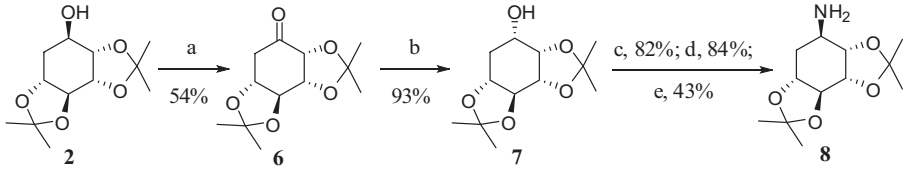

Scheme 3. Synthesis of aminoquercitol bisacetonide **8**. *Reagents and conditions*: (a) Ac_2O, DMSO; (b) $LiAlH_4$; (c) $MeSO_2Cl$, Et_3N, DMAP; (d) NaN_3, DMF, 15-crown-5-ether, 100 °C; (e) $LiAlH_4$.

cyclohexane-aminocyclitol bear better resemblance to the transition state of a glucose substrate.[15]

In our previous study, the unmodified aminoquercitols **12a** and **13a** (Fig. 2) synthesized from naturally available (+)-*proto*-quercitol (**1**) showed promising inhibition against maltase (4.4–5.8 μM) and sucrase (6.8–7.3 μM).[12] However, modification of the amino group with small hydrophobic alkyl chains such as ethyl (**12b** and **13b**) and diethyl (**12c** and **13c**) mostly reduced inhibitory potency.[12] Surprisingly, in this study, the installation of serinol moiety or propane-1,3-diol at amino group considerably enhanced the inhibition compared with the unmodified aminoquercitols **12a** and **13a**; 6–8 and 3–4 folds against maltase and sucrase, respectively. Although the propane-1,3-diol residue (C3) possesses comparable alkyl chain length with the ethyl (C2) group, the presence of two terminal hydroxyls makes products **10** and **11** more hydrophilic and more likely to participate in enhancing binding affinity to the enzyme. A docking study of **10** and **11** towards α-glucosidase was carried out and is elaborated in the next section.

To gain insight into the mechanism underlying the inhibition of the newly synthesized *N*-1,3-dihydroxypropylaminocyclitols, compound **11** was selected as a representative for kinetic study. For maltase, the Lineweaver–Burk plot of **11** in Fig. 3a revealed a series of straight lines; all of which intersect the Y-axis at a single point between 0.2 and 0.4 $(mM/min)^{-1}$. Kinetic analysis showed that K_m values increased with the concentration of compound **11** while V_{max} value remained unchanged, indicating that this compound acts as a competitive inhibitor. The K_i value of 0.29 μM (Table 2) was obtained by construction of the secondary plot of slope *vs* concentration

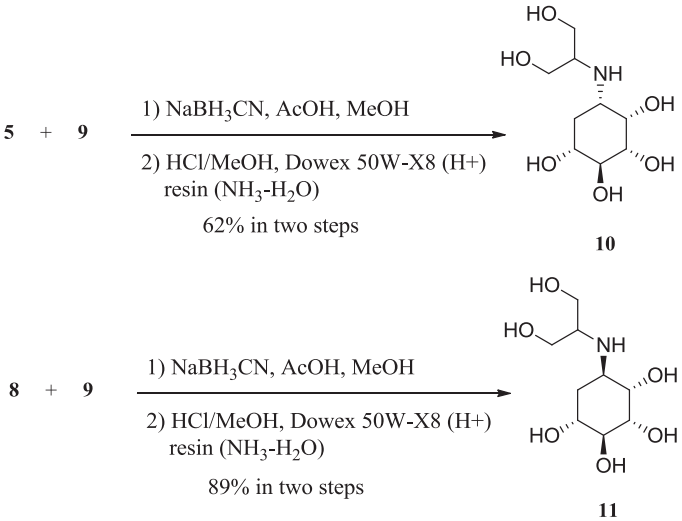

Scheme 4. Synthesis of *N*-1,3-dihydroxypropylaminocyclitols **10** and **11**.

Table 1
α-Glucosidase inhibitory effect of *N*-1,3-dihydroxypropylaminocyclitols and related analogues

Compounds	Inhibitory effect IC_{50} (μM)		
	Baker's yeast	Maltase	Sucrase
Cyclooctane-aminocyclitol[a]	NI[b]	NT	NT
Cycloheptane-aminocyclitol[a]	NI[c]	NT	NT
Cyclohexane-aminocyclitol			
10	NI	0.90	1.7
11	NI	0.57	2.1
12a	2890	5.8	7.3
12b	NI	NI	NI
12c	1600	21	360
13a	12.5	4.4	6.8
13b	1200	57	NI
13c	1600	5.0	NI
Voglibose	4300	0.25	0.094

[a] Referred to the first structure of each class appeared in Fig. 1.
[b,c] Inhibition less than 50% at highest test concentration of 1 mM (Lit. 5 and 8, respectively).

Please cite this article in press as: Wisuttaya Worawalai, Pornthep Sompornpisut, Sumrit Wacharasindhu, Preecha Phuwapraisirisan, Voglibose-inspired synthesis of new potent α-glucosidase inhibitors *N*-1,3-dihydroxypropylaminocyclitols, Carbohydrate Research (2016), doi: 10.1016/j.carres.2016.04.014

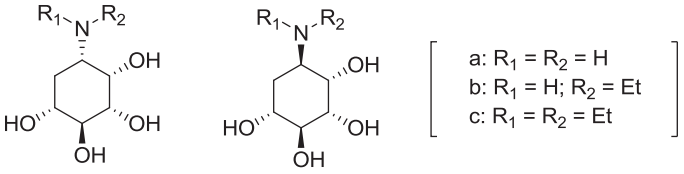

Fig. 2. Structures of aminoquercitols and *N*-alkylated analogues **12** and **13**.

Table 2
IC_{50} and K_i values of **11** and voglibose

Compound	IC_{50} (μM)		K_i (μM)		Type of inhibition
	Maltase	Sucrase	Maltase	Sucrase	
11	0.57	2.1	0.29	2.6	Competition
Voglibose	0.25	0.094	0.12[a]	0.070[a]	Competition

[a] Lit 16.

of **11** (Fig. 3a). Using similar methodology, the mode of inhibition against sucrase was also determined. Compound **11** inhibited sucrase in a competitive manner (Fig. 3b) with K_i value of 2.6 μM (Table 2). Interestingly, the inhibitory mechanism of **11** and related *N*-substituted aminoquercitols against maltase and sucrase[12] is similar to that of voglibose; however, voglibose demonstrated tighter binding.[16]

Although a variety of aminoquercitols and related analogues have been reported for their α-glucosidase inhibition, the binding between the quercitol core structure and the active site of the enzyme has never been investigated. In the present study, the binding mode between synthesized inhibitors (**10** and **11**) and maltase was first investigated by applying the validated molecular dock open-source program AutoDock Vina.[17] Initially, a homology modelled structure of rat intestinal maltase was constructed, and the docking reliability was validated using miglitol (MIG) ligand. Docking to the active site of the human N-terminal catalytic subunit of the maltase-glucoamylase (hu-ntMGAM) receptor revealed similar results to those of a previous report,[18] producing the crystallographic binding pose. Next, a three-dimensional model of the N-terminal subunit of rat maltase-glucoamylase (rat-ntMGAM) was constructed using the crystal structure of hu-ntMGAM complexed with miglitol as a template and the results are shown in Fig. 4a.

From the Ramachandran plot, the main-chain conformation for 98.8% amino acid residues, except glycine and proline, were within the allowed or most favoured regions and the overall Procheck G-factor was 0.04. The Qmean4 and Z-score of the homology model of rat-ntMGAM was 0.705 and –0.86, respectively. Both the G-factor and Qmean scores were above the threshold, suggesting the good quality of the model. Further validation of the homology model by

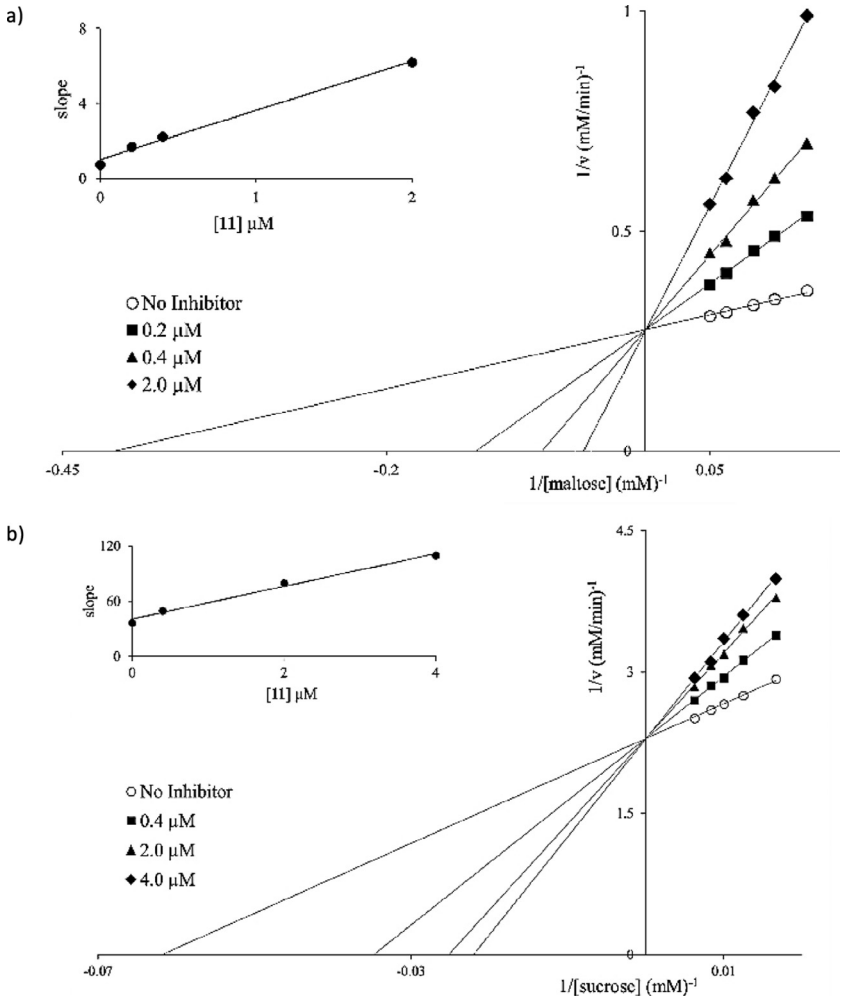

Fig. 3. Lineweaver–Burk plots for inhibitory activity of **11** against rat intestinal: (a) maltase; (b) sucrase. Inset: secondary replots of slope *vs* [I] from a primary Lineweaver–Burk plot for the determination of K_i.

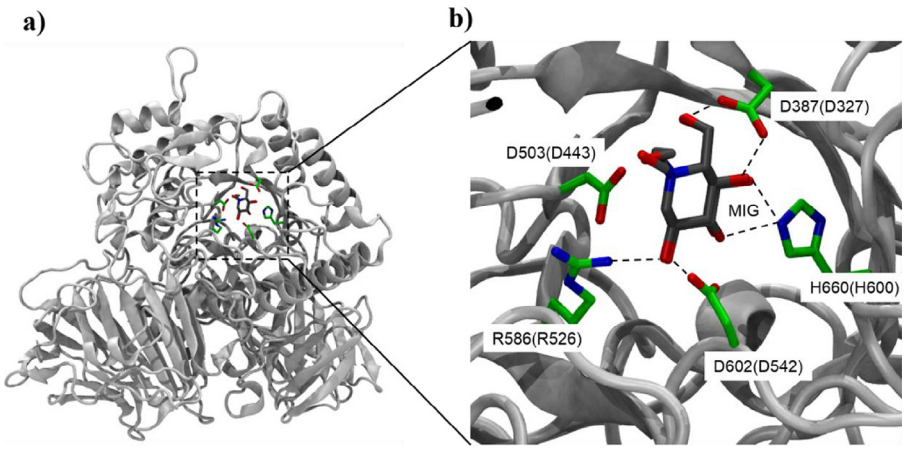

Fig. 4. (a) Homology model of the rat intestinal N-terminal domain of maltase-glucoamylase (rat-ntMGAM) and (b) Structural superimposition between the crystal and docked miglitol (RMSD = 0.48 Å). The figure also shows the conserved residues important for the binding of the inhibitor in the active site of rat-ntMGAM and hu-ntMGAM (number in parentheses). The dashed lines illustrate atom pairs within hydrogen bond distances.

docking MIG into the binding site showed that the ligand binding pose was highly similar to the one in the X-ray structure of huntMGAM (Fig. 4b), especially a significant conservation in the binding site. This includes the key conserved residues: D387, D503, D602, R586 and H660, which have been shown to make important hydrogen bonds with the inhibitor.[18]

Compounds **10**, **11**, and voglibose that had been geometrically optimized were used for the docking experiments and then for the comparison. From the docking results, voglibose, **10** and **11** have been shown to bind to the same binding site as miglitol (Fig. 5 and Fig. S16). The major interaction between the inhibitors and the enzyme was the hydrogen bond that forms between the OH groups of the cyclohexane ring (quercitol moiety) of the inhibitors and the polar or charged residues D387, D503, D602, R586 and H660 (Fig. 5a and b). Fig. 5c demonstrated the polar surface of the binding pocket of the enzyme that is complementary to the polar groups of the three inhibitors (**10**, **11**, and voglibose). As regards the binding pose of miglitol and voglibose, compounds **10** and **11** orient its cyclohexane ring in such a way to compensate similar interactions engaged by the OH groups of C3, C4, C5 and the hydroxymethyl groups (CH_2OH) with the surrounding conserved amino acids (Fig. S16 and Table S1). Interestingly, the docking results indicated that the cyclohexane ring of voglibose was more tilted than that of the miglitol. The different orientation of the two inhibitors was partly due to the configuration of the hydroxyl groups and the difference in the position of the hydroxymethyl substituent at C2 for miglitol and at C5 for voglibose. Noticeably, the hydroxymethyl group of voglibose faced towards D602 and H660 while the CH_2OH of the miglitol pointed outwards from the binding pocket. In addition, one of the OH group in the dihydroxypropane of voglibose was close enough to form a hydrogen bond to D602 whereas no apparent interaction with the enzyme was observed for the hydroxyethyl substituent of miglitol. Fig. 5d shows a comparison of the orientation of **10** against voglibose and **11** against miglitol. Apparently, the orientation of the cyclohexane ring of **10** was more similar to voglibose as the dialkoxyamino substituent of both inhibitors shared the same configuration. It should be noted that the arrangement of the cyclohexane ring of **11** in binding pocket was more similar to that of miglitol. These docking results could explain why both inhibitors exhibit a high binding affinity for rat maltase.

The vina docking scores for **10**, **11** and voglibose were –9.7, –9.9, and –12.4 kcal/mol (Table 3), respectively. These results were consistent with the experimental results (IC_{50}) showing that voglibose has slightly lower inhibitory activity against rat maltase than **10** and **11**.

In summary, new diastereomeric *N*-1,3-dihydroxypropylaminocyclitols **10** and **11** were synthesized from

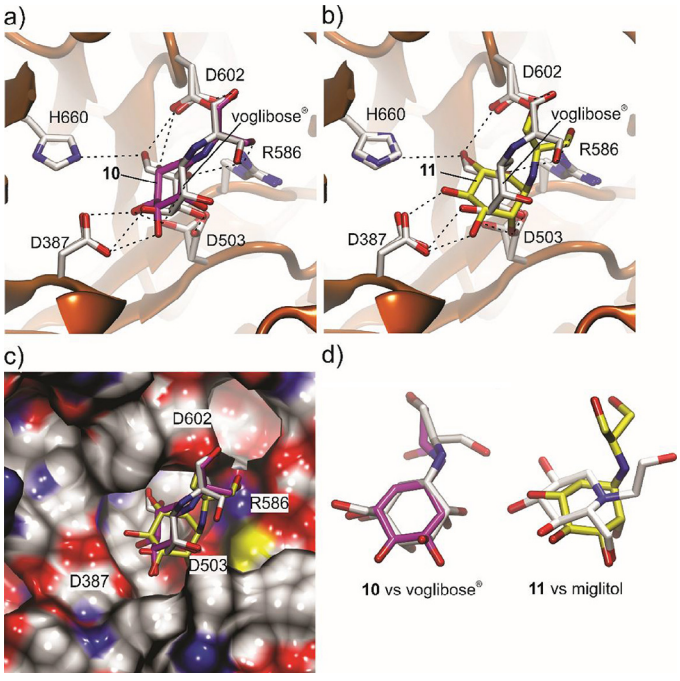

Fig. 5. The molecular docking results. Comparisons of the binding conformations of **10** (magenta) *vs* voglibose® (a), **11** (yellow) *vs* voglibose® (b), the three inhibitors in molecular surface representation (c), and the two distinct binding poses (d). The surrounding conserved residues and ligand molecules are in stick representation. Hydrogen bonds (defined according to a donor-acceptor heavy-atom distance of less than 3.4 Å) are depicted by dashed lines. (For interpretation of the references to color in this figure legend, the reader is referred to the web version of this article.)

Table 3
Inhibitory activity (IC_{50}) and Vina docking scores of **10**, **11** and voglibose

Compound	IC_{50} (μM)	Vina docking scores[a] (kcal/mol)
10	0.90	–9.7
11	0.57	–9.9
Voglibose	0.25	–12.4

[a] Calculated using AutoDock Vina from homology rat intestinal maltase.

Please cite this article in press as: Wisuttaya Worawalai, Pornthep Sompornpisut, Sumrit Wacharasindhu, Preecha Phuwapraisirisan, Voglibose-inspired synthesis of new potent α-glucosidase inhibitors *N*-1,3-dihydroxypropylaminocyclitols, Carbohydrate Research (2016), doi: 10.1016/j.carres.2016.04.014

naturally available (+)-*proto*-quercitol (**1**), through reductive amination of aminoquercitol bisacetonides (**5** and **8**) and 1,3-dihydroxyacetone dimer (**9**) as a key step. The application of **1** as a glucomimic core structure along with the modification of the amino group with *N*-1,3-dihydroxypropyl moiety led to a new pair of potent α-glucosidase inhibitors. These results contrast with other related *N*-1,3-dihydroxypropylaminocyclitols with larger rings (cycloheptane and cyclooctane), which are inactive against α-glucosidase. Therefore, the cyclohexane core structure of (+)-*proto*-quercitol (**1**) plays a superior role in exerting inhibition while the propane-1,3-diol residue reinforces binding with the active site of the enzyme.

In addition, the inhibitions of **10** and **11** were also more highly potent than those of related *N*-ethyl aminoquercitols (**12a**-**13c**). Subsequent investigation of the mechanism underlying the inhibition suggested that compound **11** inhibited rat intestinal maltase and sucrase in a competitive manner. A docking study of **10** and **11** towards maltase presented similar binding profiles with that of the antidiabetic drug voglibose, in which key hydrogen bonding such as OH cyclitol- D387, D503, and H660 were clearly observed. To our knowledge, this is the first report of the docking study of quercitol-derived compounds towards α-glucosidase. The aforementioned findings from our study could be important clues in enhancing insights into the inhibition mechanism of small molecules, particularly six-membered cyclitols, and inspiring future investigation into other *N*-1,3-dihydroxypropylaminocyclitols.

1. Experimental

1.1. General methods

All moisture-sensitive reactions were carried out under a nitrogen atmosphere. All solvents used in the reactions were distilled prior to use. HRESI-MS spectra were obtained from a micrOTOF Bruker mass spectrometer. ^{1}H and ^{13}C spectra were recorded by a Varian Mercury$^+$ 400 NMR spectrometer and the chemical shifts (δ, ppm) were reported by referencing to solvent residues. TLC profile analysis was performed on Merck silica gel 60 F_{254} plates (0.25 mm thick layer) and visualized under UV (254 nm) followed by dipping in 10% anisaldehyde or $KMnO_4$ reagents. Column chromatography was conducted using Merck silica gel 60 (70–230 mesh), Sephadex LH-20 or Dowex 50W-X8 (H+).

1.2. 1,2:3,4-Di-O-isopropylidene-5R-(+)-proto-quercitol (**2**)

To a solution of (+)-*proto*-quercitol (64 mg, 0.39 mmol) in DMF (4 mL) were added 2,2-dimethoxypropane (480 μL, 3.90 mmol) and *p*-toluenesulfonic acid monohydrate (7.4 mg, 0.039 mmol) and the mixture was stirred for 1 h at 80 °C and warmed to room temperature for 24 h. After the reaction was completed, the reaction mixture was diluted with distilled water and extracted with EtOAc (3 × 50 mL). The combined organic layers were then washed with brine, dried over Na_2SO_4, filtered and concentrated under reduced pressure. The residue was chromatographed on a silica gel column using 50% EtOAc-hexane to yield bis-acetonide **2** (71 mg, 75%) as a syrup; ^{1}H NMR ($CDCl_3$, 400 MHz) δ 4.26 (dd, *J* = 8.0, 6.4 Hz, 1H), 4.20 (ddd, *J* = 8.0, 5.6, 5.2 Hz, 1H), 4.13 (dd, *J* = 5.6, 5.6 Hz, 1H), 3.70 (ddd, *J* = 10.4, 10.2, 6.3 Hz, 1H), 3.53 (dd, *J* = 10, 8.4 Hz, 1H), 1.92–2.06 (m, 2H), 1.44 (s, 3H), 1.36 (s, 3H), 1.35 (s, 3H), 1.29 (s, 3H); ^{13}C NMR ($CDCl_3$, 100 MHz) δ 111.3, 109.8, 81.1, 79.8, 76.1, 72.1, 68.7, 32.3, 27.8, 27.0, 26.9, 25.5.

1.3. 1,2:3,4-Di-O-isopropylidene-5R-O-mesyl-(+)-proto-quercitol (**3**)

To a 273 mg (1.12 mmol) portion of **2** in CH_2Cl_2 (12 mL) was added DMAP (trace amount) and triethylamine (1.3 mL, 8.9 mmol). The mixture was cooled to 0 °C. Mesyl chloride (261 μL, 3.35 mmol) was added slowly and the mixture was stirred for 3 h at room temperature. The product was extracted with CH_2Cl_2 (3 × 50 mL), washed with brine, dried over anhydrous Na_2SO_4, filtered and concentrated under reduced pressure. The crude product was purified by silica gel chromatography (50% EtOAc-hexane) to give **3** (317 mg, 81%) as an amorphous solid; ^{1}H NMR ($CDCl_3$, 400 MHz) δ 5.03 (dt, *J* = 6.0, 5.4 Hz, 1H), 4.34 (br d, *J* = 6.0 Hz, 2H), 3.69 (dt, *J* = 10.4, 6.4 Hz, 1H), 3.60 (m, 1H), 3.07 (s, 3H), 2.31 (m, 1H), 2.21 (m, 1H), 1.50 (s, 3H), 1.41 (s, 6H), 1.34 (s, 3H).

1.4. 5S-Azido-5-deoxy-1,2:3,4-di-O-isopropylidene-(+)-proto-quercitol (**4**)

A mixture of **3** (230 mg, 0.71 mmol), sodium azide (465 mg, 7.12 mmol), 15-crown-5-ether (1.5 mL, 7.1 mmol), and DMF (7 mL) was stirred for 24 h at 100 °C. The reaction mixture was extracted with EtOAc (3 × 100 mL), washed with brine several times, dried over anhydrous Na_2SO_4, filtered and concentrated under reduced pressure. The residue was chromatographed on a column of silica gel (30% EtOAc-hexane) to give the azide **4** (152 mg, 79%) as an amorphous solid; ^{1}H NMR ($CDCl_3$, 400 MHz) δ 4.35 (dd, *J* = 4.8, 4.8 Hz, 1H), 4.14 (dd, *J* = 8.4, 5.6 Hz, 1H), 3.58–3.68 (m, 2H), 3.30 (dt, *J* = 10.6, 4.4 Hz, 1H), 2.30 (m, 1H), 1.89 (m, 1H), 1.52 (s, 3H), 1.37 (s, 3H), 1.35 (s, 3H), 1.33 (s, 3H); ^{13}C NMR ($CDCl_3$, 100 MHz) δ 111.7, 110.6, 81.0, 76.3, 76.2, 73.1, 57.2, 29.1, 27.9, 26.9, 26.8, 25.9.

1.5. 5S-Amino-5-deoxy-1,2:3,4-di-O-isopropylidene-(+)-proto-quercitol (**5**)

To a cool solution of the azide **4** (34 mg, 0.12 mmol) in THF (1.2 mL) at 0 °C was added $LiAlH_4$ (480 μL, 1 M, 0.48 mmol) dropwise. The mixture was stirred for 3 h, diluted with 1 M $NaHCO_3$, extracted by EtOAc (3 × 30 mL), washed with brine, dried over Na_2SO_4, filtered and concentrated under reduced pressure. The residue was purified by flash chromatography using 20% MeOH-EtOAc to yield an amine **5** (21 mg, 71%) as a pale yellow oil; ^{1}H NMR (CD_3OD, 400 MHz) δ 4.23 (dd, *J* = 4.8, 4.4 Hz, 1H), 4.07 (dd, *J* = 8.4, 4.8 Hz, 1H), 3.41 (dd, *J* = 9.0, 9.0 Hz, 1H), 3.30 (dt, *J* = 10.6, 3.2 Hz, 1H), 3.13 (dt, *J* = 11.6, 4.8 Hz, 1H), 2.08 (m, 1H), 1.51 (dt, *J* = 11.6, 11.6 Hz, 1H), 1.41 (s, 3H), 1.29 (s, 6H), 1.27 (s, 3H); ^{13}C NMR (CD_3OD, 100 MHz) δ 110.5, 109.0, 82.5, 77.7, 76.4, 74.1, 48.6, 32.8, 27.5, 25.8, 25.1.

1.6. 1,2:3,4-Di-O-isopropylidene-5-cyclohexanone (**6**)

To a solution of **2** (585 mg, 2.39 mmol) in DMSO (18.0 mL, 266 mmol) was added acetic anhydride (23 mL, 239 mmol) for 5 h at room temperature. The reaction mixture was extracted with EtOAc (3 × 200 mL), washed with brine several times, dried over anhydrous Na_2SO_4, filtered and concentrated under reduced pressure. The crude product was purified by silica gel column (20% EtOAc-hexane) to give **6** (317 mg, 54%) as a colourless powder; ^{1}H NMR ($CDCl_3$, 400 MHz) δ 4.59 (dd, *J* = 8.4, 8.0 Hz, 1H), 4.43 (d, *J* = 8.4 Hz, 1H), 4.07 (dt, *J* = 10.6, 6.8 Hz, 1H), 3.50 (dd, *J* = 10.4, 7.6 Hz, 1H), 2.93 (dd, *J* = 18.0, 7.2 Hz, 1H), 2.42 (dd, *J* = 18.2, 11.0 Hz, 1H), 1.44 (s, 3H), 1.42 (s, 3H), 1.40 (s, 3H), 1.32 (s, 3H); ^{13}C NMR ($CDCl_3$, 100 MHz) δ 203.6, 113.6, 112.3, 82.2, 78.7, 75.2, 70.6, 41.1, 27.1, 27.0, 26.7, 24.7.

1.7. 1,2:3,4-Di-O-isopropylidene-5S-(+)-proto-quercitol (**7**)

To a cool solution of **6** (50 mg, 0.12 mmol) in THF (2 mL) at 0 °C was added $LiAlH_4$ (825 μL, 1 M, 0.82 mmol) dropwise. The mixture was stirred for 3 h, diluted with 1 M $NaHCO_3$, extracted by EtOAc (3 × 30 mL), washed with brine, dried over Na_2SO_4, filtered and concentrated under reduced pressure. The residue was purified by flash chromatography using 50% EtOAc-hexane to yield **7** (47 mg, 93%) as an amorphous solid; ^{1}H NMR ($CDCl_3$, 400 MHz) δ 4.24–4.32 (m,

Please cite this article in press as: Wisuttaya Worawalai, Pornthep Sompornpisut, Sumrit Wacharasindhu, Preecha Phuwapraisirisan, Voglibose-inspired synthesis of new potent α-glucosidase inhibitors *N*-1,3-dihydroxypropylaminocyclitols, Carbohydrate Research (2016), doi: 10.1016/j.carres.2016.04.014

2H), 4.10 (m, 1H), 4.00 (dd, J = 10.0, 7.6 Hz, 1H), 3.45 (m, 1H), 2.36 (ddd, J = 13.2, 6.4, 6.0 Hz, 1H), 1.89 (ddd, J = 13.0, 10.8, 5.2 Hz, 1H), 1.55 (s, 3H), 1.50 (s, 3H), 1.42 (s, 3H), 1.38 (s, 3H).

1.8. 5R-Amino-5-deoxy-1,2:3,4-di-O-isopropylidene-(+)-proto-quercitol (**8**)

The synthetic procedures for **8** were similar to those described in *1.3–1.5* using **7** as starting material. **8**; colourless oil (43%); ^{1}H NMR (CD_3OD, 400 MHz) δ 4.31 (dd, J = 7.0, 7.0 Hz, 1H), 4.10 (dd, J = 6.8, 6.8 Hz, 1H), 3.79 (m, 1H), 3.68 (dd, J = 9.0, 9.0 Hz, 1H), 3.28 (m, 1H), 1.98 (m, 1H), 1.83 (m, 1H), 1.46 (s, 3H), 1.39 (s, 6H), 1.34 (s, 3H).

1.9. General procedure for the synthesis of N-1,3-dihydroxypropylaminocyclitols ***10*** and ***11***

To a solution of aminoquercitol bisacetonide **5** or **8** (1 equiv) in methanol (1.0 mL/0.1 mmol of **5** or **8**) under an atmosphere of N_2 was treated with sodium cyanoborohydride (2 equiv), acetic acid (4 μL/0.05 mmol of **5** or **8**) and 1,3-dihydroxyacetonedimer (3 equiv). After stirring at room temperature for 24 h, the reaction mixture was evaporated to dryness, further added 1.25 M methanolic HCl (1 mL) and stirred at room temperature for 4 h. The reaction mixture was filtered to remove the white precipitate and the obtained filtrate was evaporated to dryness. The crude product was redissolved with H_2O, loaded onto Dowex 50W-X8 (H^+) column and eluted with H_2O and 50% NH_3-H_2O. Fractions eluted with 50% NH_3-H_2O were evaporated to give **10** or **11**.

***N*-1,3-dihydroxypropylaminocyclitol 10**; yellow oil; $[\alpha]_D^{20} = +27.5 = +27.5$ (c 0.5, H_2O); ^{1}H NMR (D_2O, 400 MHz) δ 3.93 (br s, 1H), 3.24–3.57 (m, 7H), 2.93–3.00 (m, 2H), 1.86 (br d, J = 10.8 Hz, 1H), 1.45 (br d, J = 10.8 Hz, 1H); ^{13}C NMR (D_2O, 100 MHz) δ 74.2, 72.5, 69.8, 69.1, 60.3, 59.8, 56.9, 51.4, 31.6; HRMS m/z 238.1292 $[M+H]^+$ (calcd for $C_9H_{20}NO_6$, 238.1291).

***N*-1,3-dihydroxypropylaminocyclitol 11**; yellow oil; $[\alpha]_D^{20} = +30.8 = +30.8$ (c 0.5, H_2O); ^{1}H NMR (D_2O, 400 MHz) δ 3.82 (br s, 1H), 3.40–3.64 (m, 7H), 2.99 (br s, 1H), 2.74 (br s, 1H), 1.70–1.82 (m, 2H); ^{13}C NMR (D_2O, 100 MHz) δ 72.7, 70.0, 69.5, 67.4, 59.4, 59.2, 56.5, 52.4, 29.6; HRMS m/z 238.1284 $[M+H]^+$ (calcd for $C_9H_{20}NO_6$, 238.1291).

1.10. α-Glucosidase inhibition assay

α-Glucosidase inhibition of synthesized compounds against baker's yeast was evaluated on the basis of the *p*-nitrophenoxide colorimetric method.[12] Briefly, a 10 μL of compound (1 mg/mL in DMSO) was pre-incubated with 40 μL of α-glucosidase (0.1 U/mL in 0.1 M phosphate buffer, pH 6.9) at 37 °C for 10 min. 50 μL substrate solution (1 mM *p*-nitrophenyl-α-D-glucopyranoside, PNPG) was added to the mixture and incubated for an additional 20 min. The resulting mixture was quenched by 100 μL of 1 M Na_2CO_3. The *p*-nitrophenoxide ion released from the enzymatic reaction was determined at 405 nm by Bio-Rad 3550 microplate reader. The percentage inhibition was calculated by $[(A_0 - A_1)/A_0] \times 100$, where A_1 and A_0 are the absorbance with and without the sample, respectively. The IC_{50} value was deduced from a plot of percentage inhibition versus sample concentration. Voglibose was used as a positive control.

Inhibition against rat intestinal α-glucosidases (maltase and sucrase) was assessed using the glucose oxidase colorimetric method.[12] Basically, the powder (1 g) was homogenized with 0.9% NaCl solution (30 mL). The aliquot containing both maltase and sucrase was obtained after centrifugation (12,000 g) for 30 min. The test compound (1 mg/mL, 10 μL) was pre-incubated with crude enzyme solution (20 μL) at 37 °C for 10 min. The substrate solution (maltose: 0.58 mM, 20 μL; sucrose: 20 mM, 20 μL, respectively) in 0.1 M phosphate buffer (pH 6.9) was therefore added to the reaction mixture and incubated for an additional 40 min. The mixture was heated in an oven at 80 °C for 15 min to quench the reaction. The concentration of glucose liberated from the reaction mixture was determined by the glucose oxidase method using a commercial glucose assay kit (SU-GLLQ2, Human). The percentage inhibition was calculated using the above expression.

1.11. Kinetic study

The type of inhibition was determined by analyzing enzyme kinetic data. Maltase and sucrase activities were kept at 0.45 and 0.09 U/mg protein, respectively, in the presence of the inhibitor (concentration 0–20 μM) at various concentrations of maltose ranging from 1.0 to 20 mM. A series of V_{max} and K_m values were obtained from Y intercepts and calculated by slope × V_{max}, respectively.

1.12. Docking study

The template used for homology modelling was the human intestinal N-terminal domain of maltase-glucoamylase (hu-ntMGAM) complexed with miglitol (PDB: 3L4W). The *Rattus norvegicus* rat intestinal maltase amino acid sequence (Acc. no. XP_008761090) was retrieved from the NCBI web server after performing a BLAST search against the sequence of the template. The best match for the selected sequence of rat intestinal maltase shared an 82% sequence identity with the template sequence. The three-dimensional homology model of the rat intestinal maltase is constructed from 68 to 928 amino acid residues by the Swiss-Model Workspace server. The final protein model was obtained by energy minimization using the NAMD program.[19] The quality of the rat homology model was validated using PROCHECK and QMEAN.[19]

To investigate the binding mode of *N*-1,3-dihydroxypropylaminocyclitols and voglibose with the surrounding residues of rat intestinal maltase, the flexible docking was performed using AutoDock Vina.[17] 3D structures of all synthesized compounds (ligands) and voglibose were built and optimized at the semiempirical AM1 level using Gauss View 3.09.[20] AutoDockTools[21] were used to add polar hydrogens and compute partial the atomic charges for protein and ligands using Gasteiger charges. For ligands, all open-chain bonds were treated as active torsional bonds. The centre of the 28 × 28 × 28 Å grid box was estimated from the miglitol position present in the crystal structure. The exhaustiveness parameter was set to 64. For each compound, the docked poses that adopt an orientation similar to that of the experimental X-ray structure were chosen as a representative bound conformation. The docking results generated were analyzed using PyMOL (The PyMOL Molecular Graphics System, Version 1.5.0.4 Schrödinger, LLC) and VMD.[22]

Acknowledgments

This work (DBG5380037) was supported by the Thailand Research Fund. The postdoctoral fellowship (Ratchadaphisek Sompote Endowment Fund) to WW are gratefully acknowledged.

Appendix: Supplementary material

Supplementary data to this article can be found online at doi:10.1016/j.carres.2016.04.014.

References

1. Saito N, Sakai H, Suzuki S, Sekihara H, Yajima Y. *J Int Med Res* 1998;**26**:219.
2. Vichayanrat A, Ploybutr S, Tunlakit M, Watanakejorn P. *Diabetes Res Clin Pract* 2002;**55**:99.
3. Honjo S, Ikeda H, Kawasaki Y, Wada Y, Hamamoto Y, Aoyama T, et al. *Open Diabetes J* 2009;**2**:60.
4. Shinozaki K, Suzuki M, Ikebuchi M, Hirose J, Hara Y, Harano Y. *Metabolism* 1996;**45**:731.
5. Andriuzzi O, Gravier-Pelletier C, Bertho G, Prange T, Le Merrer Y. *Beilstein J Org Chem* 2005;**1**:1.
6. Andriuzzi O, Gravier-Pelletier C, Vogel P, Le Merrer Y. *Tetrahedron* 2005;**61**: 7094.
7. Andriuzzi O, Gravier-Pelletier C, Le Merrer Y. *Tetrahedron Lett* 2004;**45**:8043.
8. Gravier-Pelletier C, Maton W, Dintinger T, Tellier C, Le Merrer Y. *Tetrahedron* 2003;**59**:8705.
9. Gravier-Pelletier C, Maton W, Le Merrer Y. *Tetrahedron Lett* 2002;**43**:8285.
10. Gravier-Pelletier C, Maton W, Lecourt T, Le Merrer Y. *Tetrahedron Lett* 2001;**42**:4475.
11. Wacharasindhu S, Worawalai W, Rungprom W, Phuwapraisirisan P. *Tetrahedron Lett* 2009;**50**:2189.
12. Worawalai W, Wacharasindhu S, Phuwapraisirisan P. *Medchemcomm* 2012;**3**:1466.
13. Kuno S, Takahashi A, Ogawa S. *Carbohydr Res* 2013;**368**:8.
14. Albright JD, Goldman L. *J Am Chem Soc* 1967;**89**:2416.
15. Borges de Melo E, da Silveira Gomes A, Carvalho I. *Tetrahedron* 2006;**62**:10277.
16. Yoshikawa M, Morikawa T, Matsuda H, Tanabe G, Muraoka O. *Bioorg Med Chem* 2002;**10**:1547.
17. Trott O, Olson AJ. *J Comput Chem* 2010;**31**:455.
18. Sim L, Jayakanthan K, Mohan S, Nasi R, Johnston BD, Mario Pinto B, et al. *Biochemistry* 2010;**49**:443.
19. Gasteiger J, Marsili M. *Tetrahedron* 1980;**36**:3219.
20. Rinnan Å, Christensen NJ, Engelsen SB. *J Comput Aided Mol Des* 2010;**24**:17.
21. Bikadi Z, Hazai E. *J Cheminform* 2009;**1**:1.
22. Humphrey W, Dalke A, Schulten K. *J Mol Graph* 1996;**14**:33.

Please cite this article in press as: Wisuttaya Worawalai, Pornthep Sompornpisut, Sumrit Wacharasindhu, Preecha Phuwapraisirisan, Voglibose-inspired synthesis of new potent α-glucosidase inhibitors *N*-1,3-dihydroxypropylaminocyclitols, Carbohydrate Research (2016), doi: 10.1016/j.carres.2016.04.014